Drug Design, Development and Therapy

Dovepress
open access to scientific and medical research

Open Access Full Text Article

ORIGINAL RESEARCH

In silico approach for the discovery of new PPARγ modulators among plant-derived polyphenols

This article was published in the following Dove Press journal:
Drug Design, Development and Therapy
4 November 2015
Number of times this article has been viewed

José Antonio Encinar[1]
Gregorio Fernández-Ballester[1]
Vicente Galiano-Ibarra[2]
Vicente Micol[1,3]

[1]Molecular and Cell Biology Institute, [2]Physics and Computer Architecture Department, Miguel Hernández University, Elche, Spain; [3]CIBER: CB12/03/30038 Physiopathology of Obesity and Nutrition, CIBERobn, Instituto de Salud Carlos III, Palma de Mallorca, Spain

Abstract: Peroxisome proliferator-activated receptor gamma (PPARγ) is a well-characterized member of the PPAR family that is predominantly expressed in adipose tissue and plays a significant role in lipid metabolism, adipogenesis, glucose homeostasis, and insulin sensitization. Full agonists of synthetic thiazolidinediones (TZDs) have been therapeutically used in clinical practice to treat type 2 diabetes for many years. Although it can effectively lower blood glucose levels and improve insulin sensitivity, the administration of TZDs has been associated with severe side effects. Based on recent evidence obtained with plant-derived polyphenols, the present in silico study aimed at finding new selective human PPARγ (hPPARγ) modulators that are able to improve glucose homeostasis with reduced side effects compared with TZDs. Docking experiments have been used to select compounds with strong binding affinity (ΔG values ranging from −10.0±0.9 to −11.4±0.9 kcal/mol) by docking against the binding site of several X-ray structures of hPPARγ. These putative modulators present several molecular interactions with the binding site of the protein. Additionally, most of the selected compounds have favorable druggability and good ADMET properties. These results aim to pave the way for further bench-scale analysis for the discovery of new modulators of hPPARγ that do not induce any side effects.

Keywords: virtual screening, molecular docking, high-throughput computing, TZDs, human PPARγ, AutoDock/Vina, ADMET, phenolic compounds

Introduction

Human peroxisome proliferator-activated receptors (hPPARs) are nuclear soluble proteins that function as ligand-dependent transcription factors belonging to the thyroid/retinoid nuclear receptor family.[1] After binding to different types of ligands, PPARs form heterodimers with the retinoic X receptor (RXR), and the resulting PPAR/RXR heterodimer recruits different transcriptional cofactors that bind to the promoter region of the respective target gene and initiate transcription.[2] To date, three PPAR proteins have been identified:[3,4] PPARα (UniProt: Q07869-PPARA_HUMAN), PPARδ/β (UniProt: Q03181-PPARD_HUMAN), and PPARγ (UniProt: P37231-PPARG_HUMAN). All three of these proteins coordinate pathways involved in lipid and glucose metabolism. Despite the similarities in their primary and secondary structures, PPAR isoforms present marked differences in their tissue distribution, ligands, and physiological role.[5] PPARα regulates the expression of genes involved in lipid metabolism and has a higher presence in the heart, liver, and brown adipose tissue.[6] The PPARδ/β isoform is expressed ubiquitously in all tissues, particularly in tissues involved in lipid metabolism, such as adipose, liver, kidney, and muscle tissues. Based on the information currently available, it appears that PPARδ/β plays a role mainly in three areas: 1) regulation of energy metabolism, 2) cell proliferation and differentiation, and

Correspondence: José Antonio Encinar
Molecular and Cell Biology Institute, Miguel Hernández University, Edificio Torregaitán, Avenida de la Universidad, Elche 03202, Spain
Tel +34 966 65 84 53
Fax +34 966 65 87 58
Email jant.encinar@umh.es

3) protection under stress conditions, such as oxidative stress and inflammation.[7] PPARγ is the best-characterized member of the PPAR family; it is predominantly expressed in adipose tissue and plays a significant role in lipid metabolism, adipogenesis, glucose homeostasis, and insulin sensitization.[8,9] PPARγ presents two isoforms, PPARγ1 and PPARγ2, as a result of differential promoter usage and alternative splicing which results in PPARγ1 having 28 additional amino acids at the N-terminus. PPARγ1 is abundantly expressed in adipose tissue, the large intestine, and hematopoietic cells and to a lower degree in the kidneys, liver, muscles, pancreas, and small intestine. PPARγ2 is restricted to white and brown adipose tissue under physiological conditions.[10,11]

Various molecules have been suggested as biological ligands of PPARγ: polyunsaturated fatty acids, prostanoids, eicosanoids, components of oxidized low-density lipoproteins, and oxidized alkyl phospholipids.[12] These molecules can activate PPARγ and lead to increased expression of PPARγ-target genes. However, the in vivo concentration of many of these molecules is not sufficient to activate PPARγ. Therefore, further studies are needed to determine specific endogenous ligands of PPARγ. As synthetic ligands, thiazolidinediones (TZDs) are full agonists that have been used in clinical practice to treat type 2 diabetes for many years and they effectively lower blood glucose levels and improve insulin sensitivity.[13] However, the administration of TZDs has been associated with severe side effects such as fluid retention, weight gain, cardiac hypertrophy, bone fractures, and hepatotoxicity.[14] Troglitazone was withdrawn from the market due to liver toxicity; farglitazar failed to pass Phase III clinical trials due to the emergence of peripheral edema; rosiglitazone was removed from the European market due to its association with excessive cardiovascular risk. Pioglitazone is currently in clinical practice even though it has also been linked to controversial side effects, including an increased risk of cardiovascular-related death.[15] Considering these facts, it appears evident that the search for safer new agonists is an important goal in the fight against obesity-related pathologies.

The use of natural products has re-emerged in the field of drug discovery.[16] Plant-derived molecules possess a high chemical scaffold diversity, which leads to molecular promiscuity,[17] and are evolutionarily optimized to serve different biological functions, conferring them a high drug-likeness and making them an excellent source for the identification of new drug leads.[18] Several PPARγ ligands were identified in plants that are common food sources, including the tea plant, soybeans, palm oil, ginger, grapes, and wine, and a number of culinary herbs and spices[1] (eg, *Origanum vulgare*, *Rosmarinus officinalis*, *Salvia officinalis*, and *Thymus vulgaris*). The use of these compounds, which are often weak PPARγ agonists, may become an alternative for the prevention of obesity through dietary intervention. Among the natural products that have been well characterized to serve as PPARγ ligands, various phenolic compounds have been identified.[1] We recently reported[19] that the capacities of lemon verbena polyphenolic extract and its major compound verbascoside to ameliorate high glucose-induced metabolic disturbances are mediated by the PPARγ-dependent transcriptional upregulation of adiponectin. Therefore, the role of polyphenols as partial PPARγ agonists based on selective receptor–cofactor interactions and target gene regulation may deserve intensive research.[20]

The diet of Western populations is rich in phenolic compounds, which are primarily found in fruits, vegetables, and beverages, such as tea, coffee, wine, and fruit juices. However, precise knowledge of the effects of each phenolic compound on health and disease, as well as the most accurate possible assessment of polyphenol intake, still requires extensive scientific research.

In this context, we performed an in silico study to find potential efficient hPPARγ agonists from the phenolic compounds recorded in the Phenol Explorer database[21] (~924 compounds) together with other chemical libraries with molecules presenting 70% structural similarity to scutellarin (~10,437 compounds), a flavone that has been shown to bind PPAR in computational studies and has been validated in cellular assays.[22] The best scoring compounds were compared with several phytochemicals found in the literature as well-characterized PPARγ ligands. These compounds were also evaluated for their pharmacodynamic and pharmacokinetic properties. Our in silico approach aims to establish a basis for the further evaluation of potential hPPARγ modulators.

Materials and methods

Protein structures for hPPARγ and chemical libraries

To date, 130 crystal structures of the hPPARγ protein have been solved and deposited into the Protein Data Bank, many of them with their potential inhibitors, including phenolic compounds. Only the X-ray-derived PPARγ structures in complex with modulators were taken from the Brookhaven Protein Data Bank, and these have the following codes: 4PRG, 4JL4, 4JAZ, 4HEE, 4FGY, 4F9M, 4EMA, 4EM9, 4E4Q, 4E4K, 4A4W, 4A4V, 3VSP, 3VSO, 3VSP, 3VN2, 3VJI, 3V9V, and 3V9T. Altogether, these structures represent

a wide variety of sample configurations of the receptor.[23] The residues forming the binding site for the ligand were investigated.[24,25]

The two-dimensional (2D) structures of a total of 924 compounds belonging to different classes of phenolic compounds were downloaded in spatial data file (SDF) format from the Phenol Explorer 3.6 database. Additionally, the 2D structure of 10,457 scutellarin-related compounds were download in SDF format from PubChem.[26] To handle the large number of ligand structures, we developed a Python (http://www.python.org) script to convert 2D SDFs into individual three-dimensional structures in mol2 format using Marvin Suite 6.0 from ChemAxon (http://www.chemaxon.com).

Docking procedure

Prior to initiating the docking procedure, the protein (receptor) and ligand structures should be prepared. Each PDB file receptor (PPARγ) was edited using PyMOL[27] to select a single polypeptide chain and remove all water molecules and cocrystallized ligands from the binding site. All of the selected protein structures were then subjected to geometry optimization using the repair function of the FoldX algorithm.[28,29] To perform docking with AutoDock/Vina, the receptor and ligand structures were transformed to the pdbqt file format, which includes atomic charges, atom-type definitions and, for ligands, topological information (rotatable bonds).[30] These file preparations were performed using the AutoDock/Vina plugin with scripts from the AutoDock Tools package.[31] The ligands used for subsequent docking runs can be prepared either individually through PyMOL selections or by specifying a directory containing a library of ligands to be docked.[31] A grid with dimensions of 22×22×22 points was centered to ensure coverage of the binding site of the structure. The files generated for each ligand ("ligand.pdbqt" and "ligand.vina_config.txt") contain the path for "receptor.pdbqt" and "ligand.pdbqt", the coordinates of the grid center, the size of the grid in points, the path and name for one output file with all of the best calculated poses, and the path and name for another output file with the ΔG (kcal/mol) for each pose. AutoDock/Vina was set up on a Linux cluster under the ROCKS 6.1 distribution (http://www.rocksclusters.org/) with Condor Roll (http://www.rocksclusters.org/roll-documentation/condor/) to distribute all AutoDock/Vina jobs to the nodes of the cluster. AutoDock/Vina can run on a Windows OS, but should be run on a Linux OS to achieve high performance. Once the calculation is completed, two files are generated per ligand, "ligand.docked.pdbqt" and "ligand.vina.log", which contain the coordinates of the atoms for each pose (maximum of 20 poses) of a given ligand and the ΔG (kcal/mol) for each pose, respectively. When analyzing a large number of files we used a Python script to automate the reading and extraction of data from ligand.vina.log files. Compounds with minor calculated free energy variations (ie, the best theoretical binding energy) were selected as putative modulators.

In silico analysis of drug likeness and ADMET properties

The drug likeness of the screened compounds was calculated using Marvin Suite 6.0 from ChemAxon (http://www.chemaxon.com). Again, the analysis of large amounts of data was automated with a Python script to obtain up to 80 physicochemical properties of each compound. The in silico absorption, distribution, metabolism, excretion, and toxicity (ADMET) properties of the selected compounds were calculated as an alternative approach to the expensive experimental evaluation of ADMET profiles.[32] For ADMET assessment, we used admetSAR[32] and OSIRIS Property Explorer (http://www.organic-chemistry.org/prog/peo/).

Results and discussion

Cavity binding site analysis

hPPARs, particularly the hPPARγ protein, have been widely studied by crystallographers, as evidenced by the 130 X-ray structures that have been deposited in the Protein Data Bank and recorded in the UniProt database (http://www.uniprot.org/uniprot/P37231). The structural alignment of different PPARγ entries (backbone atoms of amino acids 223–505) showed root-mean-square deviation values below 0.5 Å (0.488±0.109 Å), indicating small conformational variability. All of the structures cocrystallized with a ligand present at the binding site cavity located in the area surrounding α-helix 304–330 (Figure 1A). Measurements of the volume and area of this internal cavity show a direct linear relationship with the size of the ligand, particularly the nonpolar area of the ligand (Figure 1B and Supplementary material 1). The analysis of the cavity binding site indicates that the size of the cavity is apparently adapted to the cocrystallized ligand. Because several amino acids were found to be involved in the interactions with hPPARγ ligands (modulators), the set of interacting residues should be ligand-dependent. As an example, in 3V9V.pdb, a derivative of cercosporamide,[33] which acts as a partial agonist, was cocrystalized. This ligand provides several interactions with multiple residues of the protein, including Arg280 (polar contacts)[24] and Ile262, Ile341, Ser342, Met348,

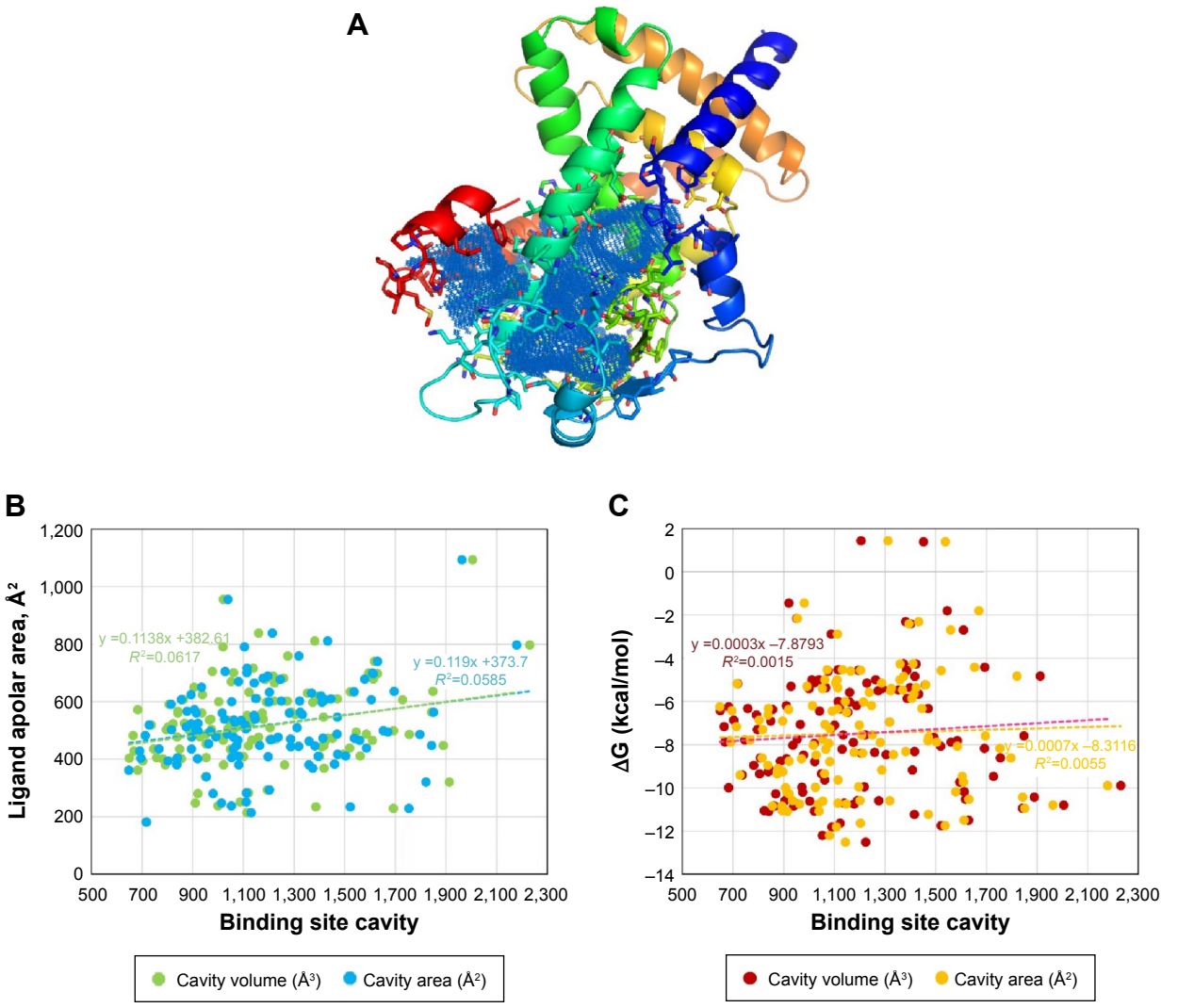

Figure 1 hPPARγ cavity binding site analysis.

Notes: Panel (**A**) shows the secondary structure of hPPARγ and large cavity of ligand binding site. Amino acids defining the cavity are displayed in sticks. The picture was created using 4PRG.pdb as an example with PyMol program.[27] Panel (**B**) shows the linear relationship between calculated[34] volume (Å³) and area (Å²) of the cavity binding site and the nonpolar surface[55] of all crystallographic ligands known to date (131 hPPARγ structures deposited into Protein Data Bank for hPPARγ). Panel (**C**) shows the linear relationship between the free energy variation calculated[30] for crystallographic ligands and the values of area and volume of the binding site. The dotted line in the graphs of the (**B**) and (**C**) panels represents the adjusted linear equation to the experimental data using Microsoft Excel software. All data are available as Supplementary material 1 in a Microsoft Excel file.

Abbreviation: hPPARγ, human peroxisome proliferator-activated receptor gamma.

Ile281, Leu353, Met343, Leu330, Tyr327, Met364, Lys367, His449, Ser289, Cys285, Arg288, Gly284, and Phe287 (nonpolar contacts).[24] In this example, the measured[34] volume and area are 971.8 Å³ and 1025.3 Å², respectively. For the remaining 130 hPPARγ structures, the size of the deep groove encompassing the binding pocket was found to be highly variable (Figure 1B and Supplementary material 1). Thus, the binding of different natural phenolic compounds and other drugs to different sites within this large internal cavity can be assumed to modulate the activity of hPPARγ, and it appears to be a promising mode of action for the design of drug candidates[35] against hPPARγ.

The variation in the free energy for the binding of ligands cocrystallized with the 123 structures of hPPARγ was measured via AutoDock/Vina (Figure 1C). Binding energies are representative of how precisely the ligand (phenolic natural products or drug candidates) binds to the target protein and were thus considered a set of reference comparisons for selection of the compounds in the library to be screened.[35] For the above-described example (3V9V.pdb), the ligand binding ΔG value measured with AutoDock/Vina was −10 kcal/mol, and only 23% of the ligands cocrystallized with hPPARγ have a ΔG≤−10 kcal/mol (Figure 1C). The calculation of the dissociation constant K_D[36] as a function of ΔG ($K_D = \exp^{\Delta G/RT}$)

indicated that ΔG values ≤−10 kcal/mol imply the K_D is in the nanomolar or subnanomolar range, which was used as a threshold to filter the docking results.

hPPARγ – ligand molecular docking analysis

Progress in high-performance computing allows the virtual screening of a large number of compounds in a short time and the selection of one of the compounds to be tested experimentally.[37] The molecular docking of a protein target and small ligand compounds predicts the best interaction mode for a defined binding site.[38,39] In the current study, hPPARγ was docked with two sets of compounds: the first contained 924 molecules registered in the Phenol Explorer database[21] as phenolic compounds, and the second set includes 10,437 compounds with structural similarity to scutellarin[22] (http://goo.gl/1O3O07), of which 1,085 comply with Lipinski's Rule of Five.[40]

X-ray crystallography techniques are commonly used to obtain conformations of proteins with high resolution and usually provide snapshots of one or some of the conformations of the proteins.[41] However, in the case of hPPARγ, there are a tremendous number of crystallographic structures that may show a large conformational space with some similarity to the native conditions of the protein. During ligand binding, the receptor protein undergoes conformational changes that are essential for its function.[42] AutoDock/Vina has been implemented to ensure flexibility of the side chains of the amino acids constituting the ligand binding site. However, performing docking while considering the flexibility of a few amino acid binding sites requires a high computational cost that cannot be assumed during the analysis of the high number of compounds used in this study. For this reason, we chose a sample of 19 hPPARγ structures (see "Materials and methods" section) for docking, and we did not consider the flexibility of the side chains of the amino acids involved in the binding sites.

Tables 1 and 2 show the docking scores obtained for phenolic compounds from the Phenol Explorer database and scutellarin-related compounds, respectively; these tables show hydrogen bonds, direct contacts based on van der Waals radii, and the ΔG calculated using AutoDocK/Vina. The free energy variation is a representative value of the number and intensity of the atomic interactions between the receptor (protein) and the ligand and can thus be considered a baseline comparison for the selection of lead compounds in the process of drug design.[35]

Table 1 includes 32 phenolic compounds with free energy variation ranging from −10.0±0.9 to −11.4±0.9 kcal/mol, which are stronger compared with the calculated ΔG values for many phenolic compounds with experimentally demonstrated affinity for hPPARγ[1] that were used as the reference set. The phenolic compounds included in Table 2 of the paper published by Wang et al[1] bind to purified hPPARγ in the micromolar range, and our calculated ΔG values for these compounds ranged from −8.8±0.7 (PE000404 – genistein) to −7.5±0.4 kcal/mol (PE000592 – resveratrol). The Δ*G* values of other polyphenols that were within this range are the following: −8.2±0.5 (PE000229 – luteolin), −8.0±0.5 (PE000291 – quercetin), −8.0±0.5 (PE000290 – kaempferol), −7.7±0.6 (PE000124 – catechin), −7.8±0.3 (PE000104 – 2′-OH-chalcone), −8.2±0.5 (PE000397 – biochanin A), −7.8±0.5 (PE000905 – 6-OH-daidzein), and −7.5±0.2 (PE000848 – 6′-OH-*O*-desmethylangolensin). Interestingly, the other 175 tested polyphenols were found to have ΔG values ranging from −9.0±0.4 to −9.9±0.7 kcal/mol (full table in Supplementary material 2), indicating that these may represent a potential source for new hPPARγ modulators. This second set of polyphenols includes scutellarin (−9.2±0.4 kcal/mol), a phenolic compound that presents antiadipogenic activity through the modulation of PPARγ in 3T3-L1 preadipocytes[22] and a reference compound that can be used to construct a structure-related chemical library that can be used in the docking experiments performed in this study.

Table 2 includes 83 scutellarin structure-related compounds (full table in Supplementary material 3) with free energy variations ranging from −10.0±0.6 to −11.0±0.6 kcal/mol; additionally, 2,772 compounds presented variations in the range of −9.0±0.6 to −9.9±0.5 kcal/mol. Among these, 179 satisfied Lipinski's Rule of Five in evaluating drug-likeness in the PubChem database (http://goo.gl/NnQ4UR), 14 compounds have been tested for biological properties (http://goo.gl/xbkcEk), and 110 compounds can be obtained from a commercial source (http://goo.gl/LTZLQ1).

Prediction of ADMET profiles

Both for the development of drugs and for the environmental risk assessment of drug candidates, it is necessary to know the ADMET properties[32] of pesticides and chemicals used in industrial chemistry. Because the experimental evaluation of ADMET is very costly and time-consuming, the application of computational techniques to predict ADMET profiles is a useful solution. The prediction of good ADMET profiles of drug candidates can help eliminate compounds with

Table 1 Molecular docking analysis for phenolic compounds showing estimated binding free energy variation[30] and interacting residues[24] of the binding site of hPPARγ

PEln	Feb (mean ± SD, kcal/mol)	H-bir	VdWir
Scutellarin	−9.21±0.40	R288	H449, E295, C285, L330, L333, S289, R288, L340, I341, I326, M364, M329, A292, Y327
PE000149	−11.44±0.93	R288	H449, E295, C285, L330, L333, S289, R288, L340, I341, I326, M364, M329, A292, Y327
PE000143	−11.19±1.05	S289, R288, S342	V339, A292, L228, L330, L333, S289, R288, L353, I341, S342, F264, I281, R280, M364, M348, G284
PE000095	−10.78±0.65	S289, R288, C285, L228	V339, L228, L330, L333, E259, Y327, H323, S289, R288, L340, I341, S342, E343, I281, R280, C285, G284, Q286, H449, I262, F264, P227, L476, I326, A292, E291
PE000086	−10.72±1.06	S289, R288, S342	I262, C285, L330, L333, S289, R288, I341, S342, F264, I281, R280, M364, M348, G284
PE000075	−10.69±0.56	C285	H449, C285, E291, L330, L333, S289, R288, E259, I326, I341, S342, F264, I281, R280, M364, M329, M348, F363, Y327
PE000515	−10.65±1.02	S289, R288, L228, S342, R280	L228, L330, G258, E259, S289, R288, I326, I341, S342, I281, R280, M364, M348, F287, K263, I262, F247, I267, H266, K265, F264, P227, I249, C285, E295, A292
PE000052	−10.62±0.94	C285	H449, C285, L330, L333, G284, S289, R288, E259, I326, I341, F264, I281, R280, M364, M348, F363, Y327
PE000281	−10.57±0.59	S289, R288, H449	H449, V339, F264, L330, L333, S289, R288, L340, I341, R280, I281, I326, M364, C285, G284, Y327
PE000058	−10.57±1.12	S289, R288, L228	K263, P227, V339, K265, A292, L228, L330, L333, S289, R288, C285, I326, I341, S342, F264, I281, M364, E295, M348, F287, E291
PE000613	−10.57±0.84	S289, R288, H449, C285, E343	L330, L333, G258, E259, V277, L255, S289, R288, L340, I341, S342, E343, I281, R280, F282, C285, F363, H449, I262, F264, I249, M348, L476, I326
PE000239	−10.54±0.80	S289, R288	V339, R280, C285, F264, L330, L333, S289, R288, L228, E259, L340, I341, S342, E343, P227, I326, M364, E295, A292, E291
PE000090	−10.46±0.92	R288, S342	F264, L333, R288, E259, I341, S342, V277, I281, R280, M329, G284
PE000370	−10.43±0.98	S289, R288	K265, A292, L330, L333, S289, R288, I326, I341, S342, F264, I281, M329, M348, G284, F287, C285
PE000385	−10.40±1.01	R288	V339, F264, L330, L333, R288, L228, I326, I341, E343, I281, M364, M329, A292, G284
PE000091	−10.39±1.01	R288, C285, S342	H449, V339, I262, C285, L330, L333, S289, R288, L340, I341, S342, F264, I281, I326, M364, M329, M348, G284, Y327
PE000787	−10.38±0.66	R288, S342	C285, F264, L330, L333, S289, R288, E259, L340, I341, S342, R280, I281, I326, M329, M348, G284, L255
PE000257	−10.37±0.69	S289, S342	K263, C285, S289, R288, E259, I267, I341, S342, F264, I281, R280, M348, G284, F287
PE000144	−10.33±0.60	R288, S342	I249, I262, C285, R288, E259, I341, S342, F264, I281, R280, M364, M348, L255
PE000089	−10.24±0.70	S289, R288, S342	L330, S289, R288, I326, I341, S342, F264, I281, R280, M364, C285
PE000286	−10.21±0.39	R288, K265, S342	V339, L330, L333, E259, R288, I341, S342, E343, I281, M364, C285, G284, F287, K263, K265, F264, P227, I249, M348, F363, L353, A292, E291
PE000824	−10.16±0.92	S289, R288, S342	V339, C285, F264, L330, S289, R288, E259, I326, I341, S342, V277, I281, R280, M364, M348, L255
PE000511	−10.15±0.75	S289, R288, S342	V339, L330, L333, E259, S289, R288, L340, I341, S342, I281, I326, M364, C285, G284, Y327, I262, F264, I249, M348, E295, A292, E291
PE000023	−10.13±1.00	S289, R288, H449	H449, V339, C285, L330, L333, S289, R288, L353, I341, S342, F264, I281, I326, M364, F282, M348, G284
PE000258	−10.11±0.73	R288, C285	I249, I262, M348, F264, G258, S289, R288, G346, E259, I341, S342, V277, I281, R280, A292, L255
PE000788	−10.08±0.45	S289, S342	C285, L330, S289, R288, I326, I341, S342, F264, I281, M364, A292
PE001043	−10.05±0.68	S342	K265, I262, F264, K263, R288, E259, I267, I341, S342, E343, R280, M348, G284, F287
PE000422	−10.05±0.54	S342	K265, R288, I262, F247, G258, K263, Q345, G346, E259, I341, S342, F264, I281, R280, C285, G284, F287, L255
PE000546	−10.04±0.65	R288, C285, S342, R280	V339, L330, E259, S289, R288, I326, I341, S342, I281, R280, M364, C285, G284, F287, K263, I262, I267, H266, K265, F264, I249, M348
PE000056	−10.03±0.56	S342	C285, L228, L330, L333, R288, E259, I341, S342, F264, I281, R280, M364, M329, A292
PE000243	−9.98±0.59	S289, S342	V339, L330, E259, S289, R288, I341, S342, I281, R280, M364, F282, C285, F363, F287, G361, K263, I262, K265, F264, M348, L356, L353, F360
PE000088	−9.98±0.98	S289, R288	L228, L330, L333, S289, R288, I326, E343, M364, C285, F363, E291

Notes: The name of each ligand has been taken from the Phenol-Explorer 3.6 database (http://phenol-explorer.eu/). A table with the data of all phenolic compounds used in the docking calculations is available as Supplementary material 2 in a Microsoft Excel file.

Abbreviations: PEln, Phenol Explorer ligand name; Feb, free energy variation for binding; H-bir, H-bonds interacting residues; VdWir, van der Waals interacting residues; hPPARγ, human peroxisome proliferator-activated receptor gamma; SD, standard deviation.

Table 2 Molecular docking analysis for scutellarin-related compounds showing estimated binding free energy variation[30] and interacting residues[24] of potential modulators compounds in the binding site of hPPARγ

Pln	Feb (mean ± SD, kcal/mol)	H-bir	VdWir
Scutellarin	−9.21±0.40	R288	H449, E295, C285, L330, L333, S289, R288, L340, I341, I326, M364, M329, A292, Y327
72358734	−10.75±0.60	S289, R288	V339, F247, I262, I249, G258, L330, L333, S289, R288, G346, E259, I326, I341, S342, I281, R280, M364, M329, A292, L255
59687997	−10.75±0.55	S289, R288	V339, L330, L333, G258, E259, Q345, S289, R288, G346, I326, I341, S342, I281, R280, M364, M329, M348, I262, F247, I249, C285, A292
59687973	−10.74±0.58	S289, R288	V339, F247, I262, I249, G258, L330, L333, S289, R288, G346, E259, I326, I341, S342, I281, R280, M364, M329, A292, L255
72358745	−10.71±0.63	S289, R288	V339, L330, L333, G258, E259, Q345, S289, R288, G346, I326, I341, S342, I281, R280, M364, M329, M348, I262, F247, I249, C285, A292
11734548	−10.45±0.58	S289, R288	I249, F247, R288, A292, G258, S289, Q345, G346, I326, I341, I262, F264, I281, M348, G284, L255
72383197	−10.44±0.65	S342	E295, C285, L330, I267, R288, E259, I326, I341, S342, F264, I281, R280, M364, M329, A292, G284
75112563	−10.43±0.69	L228	P227, I249, K265, I262, C285, F264, L330, L333, L255, R288, L228, I341, S342, E343, I281, M329, M348, G284, F287, E291
58653000	−10.42±0.60	S289, R288, S342, R280	I267, P227, T268, I262, C285, S289, R288, E259, I326, I341, S342, F264, I281, R280, P269, E295, A292, E291
58652685	−10.39±0.48	R288	F247, R288, C285, G258, L330, L333, Q345, G346, E259, I341, S342, F264, I281, R280, M348, G284, I262, L255
72383069	−10.39±0.47	R288	I249, F247, R288, C285, G258, L330, L333, Q345, G346, E259, I341, S342, F264, I281, R280, M348, G284, I262, L255
58446486	−10.37±0.94	S289, R288	V339, L228, L330, L333, L255, S289, R288, I326, I341, S342, E343, I281, M329, C285, G284, F287, I262, K265, F264, P227, I249, M348, E291
52920637	−10.37±0.74	S289	L330, G258, E259, V277, L255, Q345, S289, R288, G346, I326, I341, S342, I281, R280, M364, C285, G284, I262, F247, F264, I249, M348, F363
44258208	−10.36±0.79	R288, C285, S342	V339, L330, L333, E259, V277, M256, L255, S289, R288, L340, I341, S342, I281, R280, M364, F282, C285, F363, F360, Y327, H449, F264, M348, L356, L353, I326
45376716	−10.30±0.70	S342	E295, C285, L330, I267, R288, E259, I326, I341, S342, F264, I281, R280, M364, M329, A292, G284
73804009	−10.29±0.60	R288, S342	I249, F247, I262, A292, G258, L330, S289, R288, G346, I326, I341, S342, I281, R280, M364, M329, M348, F363, C285
75130939	−10.29±0.60	R288, S342	F247, R288, I249, G258, L330, L333, Q345, G346, E259, I341, I262, F264, I281, R280, M364, C285, G284
58446464	−10.27±0.94		V339, L330, L333, G258, E259, Q345, S289, R288, G346, I326, I341, S342, I281, R280, M364, M329, M348, I262, F247, I249, C285, A292
45783244	−10.26±0.70	R288, S342	F247, R288, I249, G258, L330, L333, Q345, G346, E259, I326, I341, I262, F264, I281, R280, M364, M329, C285, G284
72383144	−10.25±0.60	S289, S342	P227, C285, L330, L333, S289, R288, E259, I267, I341, S342, F264, I281, R280, M364, E295, A292, G284, E291
77916000	−10.24±0.65	R288, S342, R280	V339, F264, L330, L333, I267, R288, E259, L340, I341, R280, I281, I326, M329, C285, G284, H266
76788563	−10.23±0.82	C285, L228	L228, L330, L333, L255, S289, R288, I326, I341, S342, I281, M364, M329, C285, G284, F287, Y327, I262, K265, F264, P227, I249, M348, F363, E295, A292
44258121	−10.23±0.54		V339, R288, F247, G258, L330, L333, Q345, G346, E259, I326, I341, S342, F264, I281, M364, M329, I249, G284, I262, L255
58652855	−10.22±0.64	S289, S342	C285, L330, L333, S289, R288, E259, I267, I341, S342, F264, I281, R280, M364, E295, A292, G284, E291
74819302	−10.21±0.48	R288	F247, R288, A292, G258, L333, S289, Q345, G346, E259, I326, I341, S342, F264, I281, R280, M348, G284, I262, L255
25242967	−10.21±0.63	R288	C285, F264, L330, L333, P227, R288, L228, E259, I341, E343, I281, R280, M364, M348, G284, E291
73829955	−10.21±0.61	R288, S342, R280	I249, I262, M348, L333, S289, R288, E259, I267, I341, S342, F264, I281, R280, A292, G284, C285
74819395	−10.19±0.52	L228	C285, L228, L330, P227, R288, E259, I267, I341, S342, F264, I281, R280, M348, G284, E291
10929914	−10.18±0.70	S342, L228	V339, L228, L330, P227, R288, E259, I341, S342, F264, I281, R280, M364, C285, E291
25265783	−10.18±0.47	R280, S342	T268, V339, I262, A292, L330, L333, R288, E259, I267, I341, S342, F264, I281, R280, M364, M329, M348, G284, C285
75130940	−10.17±0.71	R288, S342	F247, R288, I249, G258, L330, L333, Q345, G346, E259, I326, I341, I262, F264, I281, R280, M364, M329, C285, G284
74819394	−10.17±0.89	S342	V339, L330, L333, S289, R288, I326, I341, S342, E343, I281, M364, M329, C285, F287, K263, K265, F264, P227, M348, L353, E295, A292, E291
76788584	−10.15±0.52	S289, R288, S342	L228, L330, L333, G258, E259, L255, Q345, S289, R288, G346, I341, S342, I281, R280, M329, M348, G284, K263, I262, F247, K265, F264, I249, C285, A292
42607981	−10.14±0.53	R288, C285, S342, R280	I262, C285, L228, L330, L333, R288, E259, I267, I341, S342, F264, I281, R280, M329, M348, G284

(*Continued*)

Table 2 (*Continued*)

PIn	Feb (mean ± SD, kcal/mol)	H-bir	VdWir
76788577	−10.13±1.13		V339, K265, L330, L333, R288, I326, I341, S342, F264, I281, M364, M329, C285, G284, F287, E291
75994856	−10.13±0.48	R288, C285, S342	F282, R288, C285, L330, L333, G284, S289, L356, L353, I341, S342, F264, I281, M364, M329, M348, F363, F360
3825119	−10.13±0.56	R288	V339, C285, L330, L333, R288, E259, I326, I341, S342, F264, I281, R280, M364, M329, M348, G284
78412674	−10.13±0.51	S289, C285, A292, S342	P227, C285, L330, L333, S289, R288, E259, I341, S342, F264, I281, R280, M364, E295, A292, E291
44257827	−10.12±0.54		I249, F247, R288, L255, A292, G258, L330, S289, Q345, G346, E259, I326, I341, S342, F264, I281, M364, M329, M348, I262, C285
75038437	−10.12±0.48		V339, K265, L330, L333, R288, I326, I341, S342, F264, I281, M364, M329, C285, G284, F287, E291
73829935	−10.11±0.52	R288, C285	I249, F247, R288, C285, G258, L330, L333, Q345, G346, E259, I341, S342, F264, I281, R280, M364, M348, G284, I262, L255
74819365	−10.11±0.45	R288, C285, S342	I267, P227, E295, V339, C285, L228, L330, L333, S289, R288, E259, I326, I341, S342, F264, I281, R280, M364, M329, A292
76645318	−10.10±0.67	S289, R288	L330, L333, G258, E259, V277, L255, S289, R288, G346, L340, I341, S342, I281, R280, M364, M329, M348, I262, F247, F264, I249, C285, E295, A292
58446460	−10.10±0.75	R288, S342	T268, L228, L330, L333, R288, E259, I267, I341, S342, F264, I281, R280, M364, M329, C285
76389099	−10.09±0.65	R288, S342	I267, V339, A292, L330, S289, R288, E259, I326, I341, S342, F264, I281, R280, M364, M329, M348, G284, C285
46895651	−10.09±0.54	R288	I249, F247, R288, A292, G258, L333, S289, Q345, G346, E259, I341, S342, F264, I281, R280, M348, G284, I262, L255
25242966	−10.09±0.65	A292	V339, L330, L333, S289, R288, I326, I341, S342, I281, M364, F282, C285, G284, F360, Y327, H449, K263, K265, F264, M348, F363, L356, L353, A292, E291
44258026	−10.09±0.67	S289, S342	A292, L228, L330, L333, S289, R288, L255, E259, I326, I341, S342, F264, R280, M364, M329, M348, C285
74819374	−10.08±0.99	R288, S342, R280	F264, L330, L333, E259, S289, R288, I326, I341, S342, I281, R280, M364, M329, C285, G284, I267, L228, T268, M348, E295, A292, E291
45783243	−10.08±0.48	S289, C285, A292, S342	P227, C285, L330, L333, S289, R288, E259, I341, S342, F264, I281, R280, M364, E295, A292, E291
6479876	−10.08±0.69	R288	C285, F264, L330, P227, R288, L228, E259, I341, E343, I281, R280, M364, M329, M348, G284
56658537	−10.08±0.47	R280, S342	I262, F264, L330, L333, R288, E259, I267, I341, S342, V277, I281, R280, M364, M329, I249, G284, L255
73880628	−10.08±0.74	R288, S342, R280	I267, V339, A292, L330, S289, R288, E259, I326, I341, S342, F264, I281, R280, M364, M329, M348, G284, C285
44258122	−10.08±0.50	S289, R280	I267, P227, E259, A292, F264, L330, S289, R288, L228, C285, I326, I341, E343, I281, R280, M364, M348, G284, E291
42607923	−10.08±0.67	S289, R280, S342	I267, T268, M329, I262, P227, L228, S289, R288, E259, I326, I341, S342, F264, I281, R280, P269, E295, C285, G284, E291
74412840	−10.08±1.06	R288, L228, R280	T268, E295, C285, P227, L228, L330, L333, I267, R288, E259, I326, I341, S342, F264, I281, R280, M329, A292, E291
22297406	−10.07±0.75	S289, R288, S342	I267, V339, I262, F264, L330, L333, S289, R288, E259, L340, I341, R280, I281, I326, M329, C285, G284
74978257	−10.07±0.68	R280	V339, L330, L333, E259, V277, L255, S289, R288, I326, I341, S342, I281, R280, M364, C285, G284, Y327, H449, I262, I267, F264, M348, F363, A292
74439012	−10.07±0.49		F264, L330, R288, L228, E259, I326, I341, E343, I281, R280, M364, M329, C285, G284, E291
72193650	−10.06±0.62	R280	V339, I249, C285, F264, L330, L333, I267, R288, E259, L340, I341, S342, R280, I281, I326, M329, M348, G284
73829954	−10.05±0.67	S342	I262, C285, F264, L330, P227, R288, L228, E259, I326, I341, S342, E343, I281, R280, M364, M329, M348, G284, E291
57859671	−10.05±0.76	R288, S342	T268, E295, C285, L228, L330, L333, R288, E259, I267, I341, S342, F264, I281, R280, M364, M329, A292, G284
636812	−10.04±0.60	R288, R280	V339, I249, I262, E259, A292, L330, L333, R288, C285, I267, I341, S342, F264, I281, R280, M364, E295, M348, G284, E291
75579957	−10.04±0.51	R288	V339, L228, L330, L333, L340, S289, R288, I326, I341, I281, R280, M364, F282, M348, G284, F360, F264, F226, M329, C285, F363, L356, L353, E295, A292
42607980	−10.04±0.78	S289, R288	V339, L333, G258, E259, L255, Q345, S289, R288, G346, L340, I341, S342, I281, I326, M364, C285, G284, I262, F247, F264, I249, M348
44258207	−10.03±0.62	R280	I267, V339, F264, L330, L333, G284, S289, R288, E259, L353, I341, S342, R280, I281, I326, M364, T268, C285, F363, Y327
44259194	−10.03±0.75		V339, L330, L333, E259, S289, R288, I326, I341, I281, R280, M364, F282, C285, G284, F360, Y327, F264, M348, F363, L356, L353, A292, E291
74819398	−10.03±0.65	S289, R288, C285	H449, I249, F247, R288, C285, G258, L330, S289, Q345, G346, E259, I326, I341, S342, I281, R280, M364, M348, F363, I262, Y327
21576514	−10.02±0.68	R280, S342	L330, L333, G258, E259, L255, Q345, R288, G346, I341, S342, I281, R280, M364, M348, G284, I262, F247, I267, F264, P269, T268, I249, E291
78004334	−10.02±0.57	S289, R288, S342	I267, K263, K265, E259, M348, S289, R288, C285, I326, I341, S342, F264, I281, R280, A292, G284, F287, E291

75994517	−10.01±0.61	S342	V339, G258, E259, R288, G346, I341, S342, I281, R280, M364, F282, C285, F363, F287, K263, I262, F247, I267, K265, F264, T268, I249, M348, L356, L353, F360, E291
10984998	−10.01±0.62	S342	K265, I262, F264, K263, R288, E259, I267, I341, S342, E343, I281, M348, G284, F287, L255
42607908	−10.00±0.50	S289, R288	P227, F264, L330, L333, S289, R288, L228, I326, I341, E343, I281, M364, M329, A292, G284
42607577	−10.00±0.67	R288, Y327, R280	V339, L330, L333, E259, S289, R288, I326, I341, S342, I281, R280, M364, F282, C285, F363, F360, Y327, I262, I267, F264, T268, M348, L356, L353
73981585	−9.99±0.77	R280	I267, A292, L330, S289, R288, E259, I326, I341, F264, I281, R280, M364, M329, M348, G284, C285
74412839	−9.98±0.66	R280, S342, L228	P227, T268, I262, L228, L333, I267, R288, E259, I326, I341, S342, F264, I281, R280, P269, E295, C285, G284
73802639	−9.98±0.97	R280, S342	L330, L333, G258, E259, L255, Q345, R288, G346, I341, S342, I281, R280, M364, M329, M348, G284, I262, F247, I267, F264, P269, T268, I249, E291
73079170	−9.98±0.66	S342	K265, I262, F264, K263, R288, E259, I267, I341, S342, E343, I281, R280, T268, G284, F287
56777503	−9.96±0.56		V339, F247, R288, I249, G258, L330, L333, Q345, G346, E259, I326, I341, S342, F264, I281, M364, M329, M348, G284, I262, L255
75994928	−9.96±0.64	S342	G258, E259, R288, I341, S342, I281, R280, M364, F282, C285, F363, F287, K263, I262, I267, K265, F264, P269, T268, I249, L356, L353, F360, E291
73037135	−9.95±0.64	S342	V339, K265, C285, F264, L330, L333, K263, R288, I326, I341, S342, E343, I281, M364, M329, M348, G284, F287, E291
75579959	−9.95±0.64	S289, R288	S289, K265, K263, C285, F264, L330, L333, G344, R288, L228, L353, I341, S342, E343, I281, R280, M364, M348, F363, F287, E291
74819217	−9.95±0.60	S342	L333, G258, E259, L255, Q345, R288, G346, L340, I341, S342, I281, R280, C285, G284, F287, K263, I262, F247, K265, F264, I249, M348

Notes: The name of each ligand has been taken from the PubChem database (https://pubchem.ncbi.nlm.nih.gov/). A table with the data of all PubChem compounds used in the docking calculations is available as Supplementary material 3 in a Microsoft Excel file.

Abbreviations: PIn, PubChem ligand name; Feb, free energy variation for binding; H-bir, H-bonds interacting residues; VdWir, van der Waals interacting residues; hPPARγ, human peroxisome proliferator-activated receptor gamma; SD, standard deviation.

unacceptable side effects. We calculated ADMET profiles using free online applications[32] (http://lmmd.ecust.edu.cn:8000/predict/). A limitation to the use of these applications is that the user must manually enter the chemical formula of each compound. To avoid this problem, we developed a Python script that uses the SMILE code of the compound as input and automatically obtains the calculated ADMET profile. Positive ADMET profiles for the compounds with the best calculated free energy variations (the first selection criterion) constitute a second selection criterion for the final proposed candidates of PPARγ modulators.

For ease of understanding, we present the ADMET profiles as ADME values (Tables 3 and 4 show the predicted molecular pharmacokinetic properties of the selected phenolic compounds of the Phenol Explorer database and scutellarin-related compounds, respectively) and toxicity profiles (Tables 5 and 6 show the results of the toxicity assessment of selected compounds of the Phenol Explorer database and scutellarin-related compounds, respectively). A full table with the ADME and toxicity profiles of all of the compounds used in the docking experiments is available as supplemental material (Supplementary material 2 and Supplementary material 3).

An ADME analysis includes the analysis of various properties such as ability to penetrate blood–brain barrier,[43] capability of human intestinal absorption,[43] Caco-2 permeability,[44] and abilities to function as a P-glycoprotein (P-gp) substrate[45] and inhibitor,[46,47] renal organic cation transporter,[48] and cytochrome P450 substrate[49] and inhibitor.[50]

Almost all of the selected compounds showed positive results for human intestinal absorption but negative results for blood–brain barrier and Caco-2. The selected compounds showed no inhibitory side effects in terms of renal cation transport. Analysis of the ability of the compounds to serve as P-gp substrates showed that all of the selected ligands showed positive results and were identified as noninhibitors of P-gp. This predicted behavior for the selected compounds is similar to that of other compounds that have been proven to be hPPARγ activators, such as luteolin (PE000229), quercetin (PE000291), (+)-catechin (PE000124), 2′-OH-chalcone (PE000104), biochanin A (PE000397), genistein (PE000404), and 6-OH daidzein (PE000848). Cytochromes P450 are part of a ubiquitous superfamily of hemoproteins that are involved in various metabolic pathways in humans. In this context, we focused on the potential ability of some phenolic compounds to inhibit the capacity of Cyt P450 to catalyze the oxidation of drugs and other xenobiotics.[51] These enzymes are predominantly expressed in the liver, but are also found in the small

Table 3 Predicted molecular pharmacokinetic properties of selected compounds against hPPARγ from Phenol Explorer database[21]

Compound	ADME																	
	BBB	HIA	Caco-2 permeability	Caco-2 permeability (LogPapp, cm/s)	Aqueous solubility (LogS)	P-gp substrate	P-gp inhibitor I	P-gp inhibitor II	CYP450 2C9 substrate	CYP450 2D6 substrate	CYP450 3A4 substrate	CYP450 1A2 inhibitor	CYP450 2C9 inhibitor	CYP450 2D6 inhibitor	CYP450 2C19 inhibitor	CYP450 3A4 inhibitor	CYP IP	ROCT
Scutellarin	–	+	–	–0.6443	–3.462	+	–	–	–	–	–	–	–	–	–	–	Low	–
PE000149	–	+	–	–0.2487	–3.2123	+	–	–	–	–	–	–	–	–	–	+	Low	–
PE000143	–	+	–	–1.0679	–3.3694	+	–	–	–	–	–	–	–	–	–	–	Low	–
PE000095	–	–	–	–0.5151	–2.8337	+	–	–	–	–	+	–	–	–	–	–	Low	–
PE000086	–	–	–	–0.8061	–2.6328	+	–	–	–	–	–	–	–	–	–	–	High	–
PE000075	–	–	–	–0.398	–2.935	+	–	–	–	–	+	–	–	–	–	–	Low	–
PE000515	–	–	–	–0.3752	–1.84	+	–	–	–	–	–	–	–	–	–	–	Low	–
PE000052	–	–	–	–0.5151	–2.8337	+	–	–	–	–	+	–	–	–	–	–	Low	–
PE000281	–	+	–	–1.066	–2.4368	+	–	–	–	–	–	–	–	–	–	–	Low	–
PE000058	–	–	–	–0.5151	–2.8337	+	–	–	–	–	+	–	–	–	–	–	Low	–
PE000613	–	+	–	–0.5573	–2.2303	+	–	–	–	–	–	–	–	–	–	–	High	–
PE000239	–	+	–	–0.6443	–3.462	+	–	–	–	–	–	–	–	–	–	–	Low	–
PE000090	–	–	–	–0.5756	–2.5201	+	–	–	–	–	+	–	–	–	–	–	High	–
PE000370	–	–	–	–0.5327	–2.8921	+	–	–	–	–	+	–	–	–	–	–	Low	–
PE000385	–	+	–	–0.5327	–2.8921	+	–	–	–	–	+	–	–	–	–	–	Low	–
PE000091	–	–	–	–0.8061	–2.6328	+	–	–	–	–	–	–	–	–	–	–	High	–
PE000787	–	+	–	–0.9694	–3.3193	+	–	–	–	–	–	–	–	–	–	–	Low	–
PE000257	–	+	–	–0.9863	–1.9028	+	–	–	–	–	–	–	–	–	–	–	Low	–
PE000144	–	+	–	–0.8602	–3.3141	+	–	–	–	–	–	–	–	–	–	–	Low	–
PE000089	–	–	–	–0.4745	–2.6141	+	–	–	–	–	+	–	–	–	–	–	High	–
PE000286	–	+	–	–0.7176	–2.757	+	–	–	–	–	–	–	–	–	–	–	Low	–
PE000824	–	+	–	–0.8286	–2.2638	+	–	–	–	–	–	–	–	–	–	–	Low	–
PE000511	–	–	–	–0.4946	–1.5038	+	–	–	–	–	–	–	–	–	–	–	Low	–
PE000023	–	–	–	–0.8874	–2.3343	+	–	–	–	–	–	–	–	–	–	–	Low	–
PE000258	–	+	–	–1.0492	–2.2426	+	–	–	–	–	–	–	–	–	–	–	Low	–
PE000788	–	+	–	–0.6572	–3.1192	+	–	–	–	–	–	–	–	–	–	–	Low	–
PE001043	–	+	–	–0.9634	–3.444	+	–	–	–	–	–	–	+	–	–	–	Low	–
PE000422	–	–	–	–0.7317	–2.5895	+	–	–	–	–	–	–	–	–	–	–	Low	–
PE000546	–	+	–	–0.3813	–2.6507	+	–	–	–	–	–	–	–	–	–	–	Low	–
PE000056	–	–	–	–0.7314	–2.8337	+	–	–	–	–	–	–	–	–	–	–	Low	–
PE000243	–	+	–	–0.6508	–2.7724	+	–	–	–	–	–	–	–	–	–	–	Low	–
PE000088	–	–	–	–0.7988	–2.3781	+	–	–	–	–	–	–	–	–	–	–	Low	–

Notes: Supplementary material 2 includes ADME profile for 924 compound of Phenol Explorer database. All parameters have been calculated using http://lmmd.ecust.edu.cn:8000/predict/ site.

Abbreviations: ADME, absorption distributions metabolism elimination; BBB, blood–brain barrier; HIA, human intestinal absorption; P-gp, P-glycoprotein; CYP450, cytochrome P450; CYP IP, cytochrome P450 inhibitory promiscuity; ROCT, renal organic cation transporter; hPPARγ, human peroxisome proliferator-activated receptor gamma.

Table 4 Predicted molecular pharmacokinetic properties of selected compounds against hPPARγ from scutellarin-related compounds chemical library

Compound	ADME																	
	BBB	HIA	Caco-2 permeability	Caco-2 permeability (LogPapp, cm/s)	Aqueous solubility (LogS)	P-gp substrate	P-gp inhibitor I	P-gp inhibitor II	CYP450 2C9 substrate	CYP450 2D6 substrate	CYP450 3A4 substrate	CYP450 1A2 inhibitor	CYP450 2C9 inhibitor	CYP450 2D6 inhibitor	CYP450 2C19 inhibitor	CYP450 3A4 inhibitor	CYP IP	ROCT
Scutellarin	–	+	–	–0.6443	–3.462	+	–	–	–	–	–	–	–	–	–	–	Low	–
72358734	–	+	–	–0.3119	–3.95	+	–	–	–	–	–	–	+	–	–	–	Low	–
59687997	–	+	–	–0.3119	–3.95	+	–	–	–	–	–	–	+	–	–	–	Low	–
59687973	–	+	–	–0.3119	–3.95	+	–	–	–	–	–	–	+	–	–	–	Low	–
72358745	–	+	–	–0.3119	–3.95	+	–	–	–	–	–	–	+	–	–	–	Low	–
11734548	–	+	–	0.0899	–3.9468	+	–	+	–	–	–	–	+	–	–	–	High	–
72383197	–	+	–	–0.3119	–3.95	+	–	–	–	–	–	–	+	–	–	–	Low	–
75112563	–	+	–	–0.9637	–3.2543	+	–	–	–	–	–	–	–	–	–	–	Low	–
58653000	–	+	–	–0.3119	–3.95	+	–	–	–	–	–	–	+	–	–	–	Low	–
58652685	–	+	–	–0.3119	–3.95	+	–	–	–	–	–	–	+	–	–	–	Low	–
72383069	–	+	–	–0.3119	–3.95	+	–	–	–	–	–	–	+	–	–	–	Low	–
58446486	–	+	–	–0.9637	–3.2543	+	–	–	–	–	–	–	–	–	–	–	Low	–
52920637	–	+	–	–0.3114	–3.4974	+	–	–	–	–	–	–	–	–	–	–	Low	–
44258208	–	+	–	–0.1313	–3.1698	+	–	+	–	–	–	–	–	–	–	–	Low	–
45376716	–	+	–	–0.9637	–3.2543	+	–	–	–	–	–	–	–	–	–	–	Low	–
73804009	–	+	–	–0.9415	–3.094	+	–	–	–	–	–	–	–	–	–	–	Low	–
75130939	–	+	–	–0.9415	–3.094	+	–	–	–	–	–	–	–	–	–	–	Low	–
58446464	–	+	–	–0.9637	–3.2543	+	–	–	–	–	–	–	–	–	–	–	Low	–
45783244	–	+	–	–0.9415	–3.094	+	–	–	–	–	–	–	–	–	–	–	Low	–
72383144	–	+	–	–0.3119	–3.95	+	–	–	–	–	–	–	+	–	–	–	Low	–
77916000	–	+	–	–0.9415	–3.094	+	–	–	–	–	–	–	–	–	–	–	Low	–
76788563	–	+	–	–0.9637	–3.2543	+	–	–	–	–	–	–	–	–	–	–	Low	–
44258121	–	+	–	–0.9415	–3.094	+	–	–	–	–	–	–	–	–	–	–	Low	–
58652855	–	+	–	–0.3119	–3.95	+	–	–	–	–	–	–	+	–	–	–	Low	–
74819302	+	+	–	–0.7559	–2.7909	+	–	–	–	–	–	–	–	–	–	–	Low	–
25242967	–	+	–	–0.4177	–3.1399	+	–	–	–	–	–	–	–	–	–	–	Low	–
73829955	–	+	–	–0.9415	–3.094	+	–	–	–	–	–	–	–	–	–	–	Low	–
74819395	–	+	–	–0.9415	–3.094	+	–	–	–	–	–	–	–	–	–	–	Low	–
10929914	–	+	–	–0.4714	–3.726	+	–	–	–	–	–	–	–	–	–	–	Low	–
25265783	–	+	–	–0.647	–3.2594	+	–	–	–	–	–	–	–	–	–	–	Low	–
75130940	–	+	–	–0.9415	–3.094	+	–	–	–	–	–	–	–	–	–	–	Low	–
74819394	–	+	–	–0.9415	–3.094	+	–	–	–	–	–	–	–	–	–	–	Low	–
76788584	–	+	–	–0.9637	–3.2543	+	–	–	–	–	–	–	–	–	–	–	Low	–
42607981	–	+	–	–0.9415	–3.094	+	–	–	–	–	–	–	–	–	–	–	Low	–

(*Continued*)

Table 4 (*Continued*)

Compound	ADME																	
	BBB	HIA	Caco-2 permeability	Caco-2 permeability (LogPapp, cm/s)	Aqueous solubility (LogS)	P-gp substrate	P-gp inhibitor I	P-gp inhibitor II	CYP450 2C9 substrate	CYP450 2D6 substrate	CYP450 3A4 substrate	CYP450 1A2 inhibitor	CYP450 2C9 inhibitor	CYP450 2D6 inhibitor	CYP450 2C19 inhibitor	CYP450 3A4 inhibitor	CYP IP	ROCT
76788577	–	+	–	–0.9637	–3.2543	+	–	–	–	–	–	–	–	–	–	–	Low	–
75994856	+	+	–	–0.6585	–3.736	+	–	–	–	–	–	–	–	–	–	–	Low	–
3825119	–	+	–	–0.3114	–3.3018	+	–	–	–	–	–	–	–	–	–	–	Low	–
78412674	+	+	–	–0.426	–3.9023	+	–	–	–	–	–	–	+	–	+	–	Low	–
44257827	–	+	–	–0.9415	–3.094	+	–	–	–	–	–	–	–	–	–	–	Low	–
75038437	–	+	–	–0.638	–2.8655	+	–	–	–	–	–	–	–	–	–	–	Low	–
73829935	–	+	–	–0.8798	–3.0475	+	–	–	–	–	–	–	–	–	–	–	Low	–
74819365	–	+	–	–0.9521	–2.8549	+	–	–	–	–	–	–	–	–	–	–	Low	–
76645318	–	+	–	–0.1045	–3.3068	+	–	–	–	–	+	–	–	–	–	–	Low	–
58446460	–	+	–	–0.9637	–3.2543	+	–	–	–	–	–	–	–	–	–	–	Low	–
76389099	–	+	–	–0.5903	–2.9011	+	–	+	–	–	–	–	–	–	–	–	Low	–
46895651	+	+	+	0.7197	–4.2161	+	+	+	–	–	+	–	–	–	–	–	Low	–
25242966	–	+	–	–0.647	–3.2594	+	–	–	–	–	–	–	–	–	–	–	Low	–
44258026	–	+	–	–0.1313	–3.1698	+	–	+	–	–	–	–	–	–	–	–	Low	–
74819374	–	–	–	–0.7693	–3.0348	+	–	–	–	–	–	–	–	–	–	–	Low	–
45783243	–	+	–	–0.9415	–3.094	+	–	–	–	–	–	–	–	–	–	–	Low	–
6479876	+	+	–	–0.426	–3.9023	+	–	–	–	–	–	–	+	–	+	–	Low	–
56658537	–	+	–	–0.5903	–2.9011	+	–	+	–	–	–	–	–	–	–	–	Low	–
73880628	–	+	–	–0.6917	–2.9022	+	–	–	–	–	–	–	–	–	–	–	Low	–
44258122	–	+	–	–0.6917	–2.9022	+	–	–	–	–	–	–	–	–	–	–	Low	–
42607923	–	–	–	–0.7693	–3.0348	+	–	–	–	–	–	–	–	–	–	–	Low	–
74412840	–	+	–	–0.4177	–3.1399	+	–	–	–	–	–	–	–	–	–	–	Low	–
22297406	–	+	–	–0.6917	–2.9022	+	–	–	–	–	–	–	–	–	–	–	Low	–
74978257	–	+	–	–0.4128	–3.2451	+	–	–	–	–	+	–	–	–	–	–	Low	–
74439012	–	+	–	–0.647	–3.2594	+	–	–	–	–	–	–	–	–	–	–	Low	–
72193650	–	+	–	–0.6917	2.9022	+	–	–	–	–	–	–	–	–	–	–	Low	–
73829954	–	+	–	–0.6917	–2.9022	+	–	–	–	–	–	–	–	–	–	–	Low	–
57859671	–	+	–	–0.1045	–3.3068	+	–	–	–	–	+	–	–	–	–	–	Low	–
636812	–	+	–	–0.6917	–2.9022	+	–	–	–	–	–	–	–	–	–	–	Low	–
75579957	+	+	–	–0.8161	–3.9454	+	–	–	–	–	–	–	–	–	–	–	Low	–
42607980	–	+	–	–0.9415	–3.094	+	–	–	–	–	–	–	–	–	–	–	Low	–
44258207	–	+	–	–0.2323	–2.9444	+	–	+	–	–	–	–	–	–	–	–	Low	–
44259194	–	+	–	–0.9711	–3.1116	+	–	–	–	–	–	–	–	–	–	–	Low	–
74819398	–	+	–	–0.9521	–2.8549	+	–	–	–	–	–	–	–	–	–	–	Low	–

21576514	–	+	–	–0.1313	–3.1698	+	–	+	–	–	–	–	–	–	–	–	Low	–
78004334	–	+	–	–0.2724	–2.9062	+	–	–	–	–	+	–	–	–	–	–	Low	–
75994517	+	+	–	–0.5021	–3.8832	+	–	–	–	–	–	–	–	–	–	–	Low	–
10984998	–	+	+	0.2421	–4.0211	+	–	+	–	–	–	–	+	–	–	–	High	–
42607908	–	+	–	–0.9521	–2.8549	+	–	–	–	–	–	–	–	–	–	–	Low	–
42607577	+	+	–	–0.45	–2.1632	+	–	–	–	–	–	–	–	–	–	–	Low	–
73981585	–	+	–	–0.5924	–2.8041	+	–	–	–	–	–	–	–	–	–	–	Low	–
74412839	–	+	–	–0.647	–3.2594	+	–	–	–	–	–	–	–	–	–	–	Low	–
73802639	–	+	–	–0.1313	–3.1698	+	–	+	–	–	–	–	–	–	–	–	Low	–
73079170	–	+	–	0.0899	–3.9468	+	–	+	–	–	–	–	+	–	–	–	High	–
56777503	–	+	–	–0.4128	–2.6485	+	–	–	–	–	+	–	–	–	–	–	Low	–
75994928	+	+	–	–0.5021	–3.8832	+	–	–	–	–	–	–	–	–	–	–	Low	–
73037135	–	+	–	–0.2255	–3.1749	+	–	–	–	–	+	–	–	–	–	–	Low	–
75579959	+	+	–	–0.8293	–4.0868	+	–	–	–	–	–	–	–	–	–	–	Low	–
74819217	+	–	–	–0.45	–2.1632	+	–	–	–	–	–	–	–	–	–	–	Low	–

Notes: Compound names are from PubChem database.[26] Supplementary material 3 includes ADME profile for 10,437 scutellarin-related compounds. All parameters have been calculated using the http://lmmd.ecust.edu.cn:8000/predict/ site.

Abbreviations: ADME, absorption distributions metabolism elimination; BBB, blood–brain barrier; HIA, human intestinal absorption; P-gp, P-glycoprotein; CYP450, cytochrome P450; CYP IP, cytochrome P450 inhibitory promiscuity; ROCT, renal organic cation transporter; hPPARγ, human peroxisome proliferator-activated receptor gamma.

intestine (reducing drug bioavailability), lungs, placenta, and kidneys. Five isoforms, 1A2, 2C9, 2C19, 2D6, and 3A4, are considered the most important in xenobiotic metabolism.[52] The heme group conducts reactions that are often oxidation reactions, such as aliphatic and aromatic oxidations, heteroatom oxidations and *N*- and O-dealkylations. These reactions will mainly generate more soluble compounds that are more easily excreted.[52] Most of the selected ligands (Tables 3 and 4) did not serve as substrates for all cytochrome substrates (2C9, 2D6, and 3A4), whereas some compounds (PE000095, PE000075, PE000052, PE000058, PE000090, PE000370, and PE000385) were found to act as substrates for cytochrome P450 3A4. Inhibitors of cytochrome P450 decrease the enzymatic activity of one or more cytochrome enzymes in a dose-dependent manner and promote the accumulation of drugs to toxic levels.[53] It is therefore desirable that the selected compounds do not serve as inhibitors of cytochrome P450. Most of the compounds included in Tables 3 and 4 satisfy this condition.

In the study of the prediction of toxicity profiles, several qualitative classification models, including mutagenicity,[54] tumorigenicity,[54] reproductive effectiveness,[54] irritancy,[54] human ether-a-go-go-related gene inhibition,[32] Ames toxicity,[32] carcinogenicity,[32] fish toxicity,[32] *Tetrahymena pyriformis* toxicity,[32] honey bee toxicity,[32] biodegradation,[32] acute oral toxicity category,[32] and acute rat toxicity[32] were used. Tables 5 and 6 show the toxicity profiles of the selected compounds, and Supplementary materials 2 and Supplementary materials 3 present information for all of the studied compounds. The toxicity profiles of the selected compounds revealed that most of the compounds were not mutagenic, carcinogenic, or tumorigenic. Similarly, the selected compounds were negative for Ames toxicity, weak inhibitors of human ether-a-go-go-related genes, and exhibit no properties that exert significant toxicity in humans. On the contrary, all of the selected compounds were found to present high toxicity for fish, *T. pyriformis*, and honey bees.

Conclusion

This in silico study shows that a variety of plant-derived polyphenols found in dietary sources may modulate the activity of hPPARγ more strongly than other compounds reported in the literature.[1] The compounds described in this study showed strong theoretical binding affinity (free energy variations ranging from −10.0±0.9 to −11.4±0.9 kcal/mol), as determined by docking against the binding site of several X-ray structures of hPPARγ. These putative modulators presented several molecular interactions (Tables 1 and 2)

Table 5 Predicted toxicity assessment of selected compounds against hPPARγ from Phenol Explorer database[21]

Compound	Toxicity profile														
	Mutagenic[a]	Tumorigenic[a]	Re[a]	Irritant[a]	HEaggRGI I[b]	HEaggRGI I[b]	AMES toxicity[b]	Carcinogens[b]	FT (pLC_{50}, mg/L)[b]	TPT ($pIGC_{50}$, µg/L)[b]	Honey bee toxicity[b]	Biodegradation[b]	Acute oral toxicity[b]	Carcinogenicity (three-class)[b]	RAT (LD_{50}, mol/kg)[b]
Scutellarin	None	None	None	None	Weak	–	–	–	High, 0.5766	High, 0.8765	High	–	II	Nonrequired	2.7357
PE000149	None	None	None	None	Weak	–	–	–	High, 0.8879	High, 0.5562	High	–	IV	Nonrequired	2.4019
PE000143	None	None	None	None	Weak	–	–	–	High, 0.795	High, 0.7168	High	–	IV	Nonrequired	2.6693
PE000095	None	None	None	None	Weak	–	–	–	High, 0.5839	High, 0.817	High	–	III	Nonrequired	2.6968
PE000086	None	None	None	None	Weak	–	–	–	High, 0.4549	High, 0.7176	High	–	III	Nonrequired	2.7538
PE000075	None	None	None	None	Weak	–	–	–	High, 0.5525	High, 0.8199	High	–	III	Nonrequired	2.8383
PE000515	None	None	None	None	Weak	–	–	–	High, 1.0377	High, 0.6313	High	–	III	Nonrequired	2.4319
PE000052	None	None	None	None	Weak	–	–	–	High, 0.5839	High, 0.817	High	–	III	Nonrequired	2.6968
PE000281	None	None	None	None	Weak	–	–	–	High, 0.9993	High, 0.3809	High	–	III	Nonrequired	2.7255
PE000058	None	None	None	None	Weak	–	–	–	High, 0.5839	High, 0.817	High	–	III	Nonrequired	2.6968
PE000613	None	None	None	None	Weak	–	–	–	High, 1.3132	High, 0.2999	High	–	III	Nonrequired	2.5151
PE000239	None	None	None	None	Weak	–	–	–	High, 0.5766	High, 0.8765	High	–	II	Nonrequired	2.7357
PE000090	None	None	None	None	Weak	–	–	–	High, 0.4443	High, 0.7266	High	–	III	Nonrequired	2.8163
PE000370	None	None	None	None	Weak	–	–	–	High, 0.7803	High, 0.581	High	–	III	Nonrequired	2.6133
PE000385	None	None	None	None	Weak	–	–	–	High, 0.7803	High, 0.581	High	–	III	Nonrequired	2.6133
PE000091	None	None	None	None	Weak	–	–	–	High, 0.4549	High, 0.7176	High	–	III	Nonrequired	2.7538
PE000787	None	None	None	None	Weak	–	–	–	High, 0.9957	High, 0.6702	High	–	IV	Nonrequired	2.4103
PE000257	None	None	None	None	Weak	–	–	–	High, 1.0289	High, 0.5049	High	–	III	Nonrequired	2.7026
PE000144	None	None	None	None	Weak	–	–	–	High, 0.726	High, 0.6679	High	–	IV	Nonrequired	2.6643
PE000089	None	None	None	None	Weak	–	–	–	High, 0.3962	High, 0.7186	High	–	III	Nonrequired	2.9831
PE000286	None	None	None	None	Weak	–	–	–	High, 1.035	High, 0.5666	High	–	III	Nonrequired	2.6398
PE000824	None	None	None	None	Weak	–	+	–	High, 1.1967	High, 0.2451	High	–	III	Nonrequired	2.0375
PE000511	None	None	None	None	Weak	–	–	–	High, 1.0121	High, 0.5418	High	–	III	Nonrequired	2.3222
PE000023	None	None	None	None	Weak	–	–	–	High, 1.3696	High, 0.1194	High	–	III	Nonrequired	1.9817
PE000258	None	None	None	None	Weak	–	–	–	High, 1.1013	High, 0.4888	High	–	III	Nonrequired	2.8818
PE000788	None	None	None	None	Weak	–	–	–	High, 1.0585	High, 0.7946	High	–	III	Nonrequired	2.2375
PE001043	None	None	None	None	Weak	–	–	–	High, –0.4159	High, 0.956	High	–	III	Nonrequired	3.2733
PE000422	None	None	None	None	Weak	–	–	–	High, 0.9612	High, 0.6349	High	–	III	Nonrequired	2.4798
PE000546	None	None	None	None	Weak	–	–	–	High, –0.3223	High, 1.1936	High	–	III	Nonrequired	2.679
PE000056	None	None	None	None	Weak	–	–	–	High, 0.9981	High, 0.4333	High	–	III	Nonrequired	2.2818
PE000243	None	None	None	None	Weak	–	–	–	High, 0.8074	High, 0.5411	High	–	III	Nonrequired	2.4984
PE000088	None	None	None	None	Weak	–	–	–	High, 0.7642	High, 0.5063	High	–	III	Nonrequired	2.5566

Notes: [a]These parameters were calculated using OSIRIS property explorer (http://www.organic-chemistry.org/prog/peo/). [b]These parameters were calculated using http://lmmd.ecust.edu.cn:8000/predict/ site. Supplementary material 2 includes toxicity profile for 924 compound of Phenol Explorer database.

Abbreviations: Re, reproductive effectiveness; HEaggRGI I, human ether-a-go-go-related gene inhibition I; HEaggRGI II, human ether-a-go-go-related gene inhibition II; FT, fish toxicity; TPT, *Tetrahymena pyriformis* toxicity; RAT, rat acute toxicity; LD_{50}, amount of a compound, given all at once, which causes the death of 50% (one half) of a group of test rats; hPPARγ, human peroxisome proliferator-activated receptor gamma.

Table 6 Predicted toxicity assessment of selected compounds against hPPARγ from scutellarin-related chemical library

Compound	Toxicity profile														
	Mutagenic[a]	Tumorigenic[a]	Re[a]	Irritant[a]	HEaggRGI I[b]	HEaggRGI I[b]	AMES toxicity[b]	Carcinogens[b]	FT (pLC_{50}, mg/L)[b]	TPT ($pIGC_{50}$, μg/L)[b]	Honey bee toxicity[b]	Biodegradation[b]	Acute oral toxicity[b]	Carcinogenicity (three-class)[b]	RAT (LD_{50}, mol/kg)[b]
Scutellarin	None	None	None	None	Weak	–	–	–	High, 0.5766	High, 0.8765	High	–	II	Nonrequired	2.7357
72358734	None	None	None	None	Weak	–	–	–	High, –0.0897	High, 1.2052	High	–	III	Nonrequired	2.8804
59687997	None	None	None	None	Weak	–	–	–	High, –0.0897	High, 1.2052	High	–	III	Nonrequired	2.8804
59687973	None	None	None	None	Weak	–	–	–	High, –0.0897	High, 1.2052	High	–	III	Nonrequired	2.8804
72358745	None	None	None	None	Weak	–	–	–	High, –0.0897	High, 1.2052	High	–	III	Nonrequired	2.8804
11734548	None	None	None	None	Weak	–	–	–	High, 0.1958	High, 1.355	High	–	III	Nonrequired	2.8906
72383197	None	None	None	None	Weak	–	–	–	High, –0.0897	High, 1.2052	High	–	III	Nonrequired	2.8804
75112563	None	None	None	None	Weak	–	–	–	High, 0.7137	High, 1.1182	High	–	I	Nonrequired	3.2793
58653000	None	None	None	None	Weak	–	–	–	High, –0.0897	High, 1.2052	High	–	III	Nonrequired	2.8804
58652685	None	None	None	None	Weak	–	–	–	High, –0.0897	High, 1.2052	High	–	III	Nonrequired	2.8804
72383069	None	None	None	None	Weak	–	–	–	High, –0.0897	High, 1.2052	High	–	III	Nonrequired	2.8804
58446486	None	None	None	None	Weak	–	–	–	High, 0.7137	High, 1.1182	High	–	I	Nonrequired	3.2793
52920637	None	None	None	None	Weak	–	–	–	High, 0.6766	High, 0.8401	High	–	III	Nonrequired	2.5458
44258208	None	None	None	None	Weak	–	–	–	High, 0.3454	High, 1.0989	High	–	III	Nonrequired	2.7831
45376716	None	None	None	None	Weak	–	–	–	High, 0.7137	High, 1.1182	High	–	I	Nonrequired	3.2793
73804009	None	None	None	None	Weak	–	–	–	High, 0.4122	High, 0.8952	High	–	III	Nonrequired	2.8825
75130939	None	None	None	None	Weak	–	–	–	High, 0.4122	High, 0.8952	High	–	III	Nonrequired	2.8825
58446464	None	None	None	None	Weak	–	–	–	High, 0.7137	High, 1.1182	High	–	I	Nonrequired	3.2793
45783244	None	None	None	None	Weak	–	–	–	High, 0.4122	High, 0.8952	High	–	III	Nonrequired	2.8825
72383144	None	None	None	None	Weak	–	–	–	High, –0.0897	High, 1.2052	High	–	III	Nonrequired	2.8804
77916000	None	None	None	None	Weak	–	–	–	High, 0.4122	High, 0.8952	High	–	III	Nonrequired	2.8825
76788563	None	None	None	None	Weak	–	+	–	High, 0.7137	High, 1.1182	High	–	I	Nonrequired	3.2793
44258121	None	None	None	None	Weak	–	–	–	High, 0.4122	High, 0.8952	High	–	III	Nonrequired	2.8825
58652855	None	None	None	None	Weak	–	–	–	High, –0.0897	High, 1.2052	High	–	III	Nonrequired	2.8804
74819302	None	None	None	None	Weak	–	–	–	High, –0.0832	High, 0.8121	High	–	III	Nonrequired	2.9961
25242967	None	None	None	None	Weak	–	–	–	High, 0.257	High, 0.7195	High	–	III	Nonrequired	3.001
73829955	None	None	None	None	Weak	–	–	–	High, 0.4122	High, 0.8952	High	–	III	Nonrequired	2.8825
74819395	None	None	None	None	Weak	–	–	–	High, 0.4122	High, 0.8952	High	–	III	Nonrequired	2.8825
10929914	None	None	None	None	Weak	–	–	–	High, 0.1733	High, 1.2094	High	–	III	Nonrequired	2.706
25265783	None	None	None	None	Weak	–	–	–	High, 0.1812	High, 0.6914	High	–	III	Nonrequired	3.1648
75130940	None	None	None	None	Weak	–	–	–	High, 0.4122	High, 0.8952	High	–	III	Nonrequired	2.8825
74819394	None	None	None	None	Weak	–	–	–	High, 0.4122	High, 0.8952	High	–	III	Nonrequired	2.8825
76788584	None	None	None	None	Weak	–	–	–	High, 0.7137	High, 1.1182	High	–	I	Nonrequired	3.2793
42607981	None	None	None	None	Weak	–	–	–	High, 0.4122	High, 0.8952	High	–	III	Nonrequired	2.8825
76788577	None	None	None	None	Weak	–	–	–	High, 0.7137	High, 1.1182	High	–	I	Nonrequired	3.2793
75994856	None	None	None	None	Weak	–	–	–	High, 0.3803	High, 0.785	High	–	III	Nonrequired	3.3046
3825119	None	None	None	None	Weak	–	–	–	High, 0.7319	High, 1.0022	High	–	III	Nonrequired	2.5896
78412674	None	None	None	None	Weak	–	–	–	High, –0.0293	High, 1.1449	High	–	II	Nonrequired	3.0214

(*Continued*)

Table 6 (*Continued*)

Compound	Toxicity profile													
	Mutagenic[a]	Tumorigenic[a]	Re[a]	Irritant[a]	HEaggRGI I[b]	HEaggRGI I[b]	AMES toxicity[b]	Carcinogens[b]	FT (pLC_{50}, mg/L)[b]	TPT ($pIGC_{50}$, ug/L)[b]	Honey bee toxicity[b]	Biodegradation[b]	Acute oral toxicity[b]	Carcinogenicity (three-class)[b]	RAT (LD_{50}, mol/kg)[b]
44257827	None	None	None	None	Weak	–	–	–	High, 0.4122	High, 0.8952	High	–	III	Nonrequired	2.8825
75038437	None	None	None	None	Weak	–	–	–	High, 0.8895	High, 0.5527	High	–	III	Nonrequired	2.6408
73829935	None	None	None	None	Weak	–	–	–	High, 0.8677	High, 0.5539	High	–	III	Nonrequired	2.7452
74819365	None	None	None	None	Weak	–	–	–	High, 0.7363	High, 0.6251	High	–	III	Nonrequired	2.7048
76645318	None	None	None	None	Weak	–	–	–	High, 0.5203	High, 0.7729	High	–	III	Nonrequired	2.8815
58446460	None	None	None	None	Weak	–	–	–	High, 0.7137	High, 1.1182	High	–	I	Nonrequired	3.2793
76389099	None	None	None	None	Weak	–	–	–	High, 0.5623	High, 0.7513	High	–	III	Nonrequired	2.6556
46895651	None	None	None	None	Weak	–	–	–	High, 0.3736	High, 0.8618	High	–	II	Nonrequired	3.875
25242966	None	None	None	None	Weak	–	–	–	High, 0.1812	High, 0.6914	High	–	III	Nonrequired	3.1648
44258026	None	None	None	None	Weak	–	–	–	High, 0.3454	High, 1.0989	High	–	III	Nonrequired	2.7831
74819374	None	None	None	None	Weak	–	–	–	High, 0.5473	High, 0.6801	High	–	III	Nonrequired	3.0254
45783243	None	None	None	None	Weak	–	–	–	High, 0.4122	High, 0.8952	High	–	III	Nonrequired	2.8825
6479876	None	None	None	None	Weak	–	–	–	High, –0.0293	High, 1.1449	High	–	II	Nonrequired	3.0214
56658537	None	None	None	None	Weak	–	–	–	High, 0.5623	High, 0.7513	High	–	III	Nonrequired	2.6556
73880628	None	None	None	None	Weak	–	–	–	High, 0.4422	High, 0.9205	High	–	III	Nonrequired	2.8211
44258122	None	None	None	None	Weak	–	–	–	High, 0.4422	High, 0.9205	High	–	III	Nonrequired	2.8211
42607923	None	None	None	None	Weak	–	–	–	High, 0.5473	High, 0.6801	High	–	III	Nonrequired	3.0254
74412840	None	None	None	None	Weak	–	–	–	High, 0.257	High, 0.7195	High	–	III	Nonrequired	3.001
22297406	None	None	None	None	Weak	–	–	–	High, 0.4422	High, 0.9205	High	–	III	Nonrequired	2.8211
74978257	None	None	None	None	Weak	–	–	–	High, 0.4502	High, 0.9872	High	–	III	Nonrequired	3.0446
74439012	None	None	None	None	Weak	–	–	–	High, 0.1812	High, 0.6914	High	–	III	Nonrequired	3.1648
72193650	None	None	None	None	Weak	–	–	–	High, 0.4422	High, 0.9205	High	–	III	Nonrequired	2.8211
73829954	None	None	None	None	Weak	–	–	–	High, 0.4422	High, 0.9205	High	–	III	Nonrequired	2.8211
57859671	None	None	None	None	Weak	–	–	–	High, 0.5203	High, 0.7729	High	–	III	Nonrequired	2.8815
636812	None	None	None	None	Weak	–	–	–	High, 0.4422	High, 0.9205	High	–	III	Nonrequired	2.8211
75579957	None	None	None	None	Weak	–	–	–	High, 0.4331	High, 0.8693	High	–	III	Nonrequired	3.1475
42607980	None	None	None	None	Weak	–	–	–	High, 0.4122	High, 0.8952	High	–	III	Nonrequired	2.8825
44258207	None	None	None	None	Weak	–	–	–	High, 0.5467	High, 0.8373	High	–	III	Nonrequired	2.6137
44259194	None	None	None	None	Weak	–	–	–	High, 0.3116	High, 0.9333	High	–	III	Nonrequired	2.6647
74819398	None	None	None	None	Weak	–	–	–	High, 0.7363	High, 0.6251	High	–	III	Nonrequired	2.7048
21576514	None	None	None	None	Weak	–	–	–	High, 0.3454	High, 1.0989	High	–	III	Nonrequired	2.7831
78004334	None	None	None	None	Weak	–	–	–	High, 0.8594	High, 0.6919	High	–	III	Nonrequired	2.7287
75994517	None	None	None	None	Weak	–	–	–	High, 0.6197	High, 0.9017	High	–	III	Nonrequired	3.3033
10984998	None	None	None	None	Weak	–	–	–	High, 0.2453	High, 1.2941	High	–	III	Nonrequired	2.9952
42607908	None	None	None	None	Weak	–	–	–	High, 0.7363	High, 0.6251	High	–	III	Nonrequired	2.7048

42607577	None	None	None	None	Weak	–	–	–	High, 0.1287	High, 0.8537	High	–	III	Nonrequired	2.9438
73981585	None	None	None	None	Weak	–	–	–	High, 1.0595	High, 0.5675	High	–	III	Nonrequired	2.3366
74412839	None	None	None	None	Weak	–	–	–	High, 0.1812	High, 0.6914	High	–	III	Nonrequired	3.1648
73802639	None	None	None	None	Weak	–	–	–	High, 0.3454	High, 1.0989	High	–	III	Nonrequired	2.7831
73079170	None	None	None	None	Weak	–	–	–	High, 0.1958	High, 1.355	High	–	III	Nonrequired	2.8906
56777503	None	None	None	None	Weak	–	–	–	High, 0.8428	High, 0.5803	High	–	III	Nonrequired	2.6228
75994928	None	None	None	None	Weak	–	–	–	High, 0.6197	High, 0.9017	High	–	III	Nonrequired	3.3033
73037135	None	None	None	None	Weak	–	–	–	High, 0.8824	High, 0.7073	High	–	III	Nonrequired	2.7704
75579959	None	None	None	None	Weak	–	–	–	High, 0.2054	High, 0.8567	High	–	III	Nonrequired	3.5153
74819217	None	None	None	None	Weak	–	–	–	High, 0.1287	High, 0.8537	High	–	III	Nonrequired	2.9438

Notes: Compound names are from PubChem database.[26] Supplementary material 3 include toxicity profile for 10,437 scutellarin-related compounds. [a]These parameters were calculated using OSIRIS property explorer (http://www.organic-chemistry.org/prog/peo/). [b]These parameters were calculated using http://lmmd.ecust.edu.cn:8000/predict/ site.

Abbreviations: Re, reproductive effectiveness; HEaggRGI I, human ether-a-go-go-related gene inhibition I; HEaggRGI II, human ether-a-go-go-related gene inhibition II; FT, fish toxicity; TPT, *Tetrahymena pyriformis* toxicity; RAT, rat acute toxicity; LD_{50}, amount of a compound, given all at once, which causes the death of 50% (one half) of a group of test rats; hPPARγ, human peroxisome proliferator-activated receptor gamma.

with the binding site of the protein. Additionally, most of the selected compounds present favorable druggability and good ADMET properties.

Taken together, the results of this computational study suggest that numerous plant-derived phenolic compounds, as well as other scutellarin-related compounds, can modulate the activity of hPPARγ. Although further cellular and in vivo investigations are required to confirm the physiological relevance of these results, these data highlight the potential of several phenolic compounds to become selective hPPARγ modulators able to alleviate obesity-related pathologies with reduced side effects compared with TZDs.

Acknowledgments

We thank Dr Javier Manuel Gozalvez-Sempere for allowing the use of facilities in the Linux cluster illice.umh.es. This work was partly supported by grants BFU2011-25920, AGL2014-51773-C3-1-R, and AGL2015-67995-C3-1-R from the Spanish MICINN, PROMETEO/2012/007 and ACOMP/2013/093 grants from Generalitat Valenciana, and CIBER (CB12/03/30038, Fisiopatología de la Obesidad y la Nutrición, CIBERobn, Instituto de Salud Carlos III).

Disclosure

The authors report no conflicts of interest in this work.

References

1. Wang L, Waltenberger B, Pferschy-Wenzig EM, et al. Natural product agonists of peroxisome proliferator-activated receptor gamma (PPARgamma): a review. *Biochem Pharmacol.* 2014;92(1):73–89.
2. Yu S, Reddy JK. Transcription coactivators for peroxisome proliferator-activated receptors. *Biochim Biophys Acta.* 2007;1771(8):936–951.
3. Issemann I, Green S. Activation of a member of the steroid hormone receptor superfamily by peroxisome proliferators. *Nature.* 1990; 347(6294):645–650.
4. Dreyer C, Krey G, Keller H, Givel F, Helftenbein G, Wahli W. Control of the peroxisomal beta-oxidation pathway by a novel family of nuclear hormone receptors. *Cell.* 1992;68(5):879–887.
5. Evans RM, Barish GD, Wang YX. PPARs and the complex journey to obesity. *Nat Med.* 2004;10(4):355–361.
6. Reddy JK, Hashimoto T. Peroxisomal beta-oxidation and peroxisome proliferator-activated receptor alpha: an adaptive metabolic system. *Annu Rev Nutr.* 2001;21:193–230.
7. Attianese GMPG, Desvergne B. Integrative and systemic approaches for evaluating PPARbeta/delta (PPARD) function. *Nucl Recept Signal.* 2015;13:e001.
8. Semple RK, Chatterjee VK, O'Rahilly S. PPAR gamma and human metabolic disease. *J Clin Invest.* 2006;116(3):581–589.
9. Higgins LS, Mantzoros CS. The development of INT131 as a selective PPARgamma modulator: approach to a safer insulin sensitizer. *PPAR Res.* 2008;2008:936906.
10. Auboeuf D, Rieusset J, Fajas L, et al. Tissue distribution and quantification of the expression of mRNAs of peroxisome proliferator-activated receptors and liver X receptor-alpha in humans: no alteration in adipose tissue of obese and NIDDM patients. *Diabetes.* 1997; 46(8):1319–1327.

11. Medina-Gomez G, Gray SL, Yetukuri L, et al. PPAR gamma 2 prevents lipotoxicity by controlling adipose tissue expandability and peripheral lipid metabolism. *PLoS Genet.* 2007;3(4):e64.
12. Choi SS, Park J, Choi JH. Revisiting PPARgamma as a target for the treatment of metabolic disorders. *BMB Rep.* 2014;47(11): 599–608.
13. Elte JW, Blickle JF. Thiazolidinediones for the treatment of type 2 diabetes. *Eur J Int Med.* 2007;18(1):18–25.
14. Ahmadian M, Suh JM, Hah N, et al. PPARgamma signaling and metabolism: the good, the bad and the future. *Nat Med.* 2013;19(5): 557–566.
15. Petersen RK, Christensen KB, Assimopoulou AN, et al. Pharmacophore-driven identification of PPARgamma agonists from natural sources. *J Comput Aided Mol Des.* 2011;25(2):107–116.
16. Harvey AL, Edrada-Ebel R, Quinn RJ. The re-emergence of natural products for drug discovery in the genomics era. *Nat Rev Drug Discov.* 2015;14(2):111–129.
17. Barrajon-Catalan E, Herranz-Lopez M, Joven J, et al. Molecular promiscuity of plant polyphenols in the management of age-related diseases: far beyond their antioxidant properties. *Adv Exp Med Biol.* 2014;824:141–159.
18. Cragg GM, Newman DJ. Natural products: a continuing source of novel drug leads. *Biochim Biophys Acta.* 2013;1830(6):3670–3695.
19. Herranz-Lopez M, Barrajon-Catalan E, Segura-Carretero A, Menendez JA, Joven J, Micol V. Lemon verbena (Lippia citriodora) polyphenols alleviate obesity-related disturbances in hypertrophic adipocytes through AMPK-dependent mechanisms. *Phytomedicine.* 2015;22(6):605–614.
20. Higgins LS, Depaoli AM. Selective peroxisome proliferator-activated receptor gamma (PPARgamma) modulation as a strategy for safer therapeutic PPARgamma activation. *Am J Clin Nutr.* 2010; 91(1):267S–272S.
21. Rothwell JA, Perez-Jimenez J, Neveu V, et al. Phenol-Explorer 3.0: a major update of the Phenol-Explorer database to incorporate data on the effects of food processing on polyphenol content. *Database.* 2013;2013:bat070.
22. Lu K, Han M, Ting HL, Liu Z, Zhang D. Scutellarin from *Scutellaria baicalensis* suppresses adipogenesis by upregulating PPARalpha in 3T3-L1 cells. *J Nat Prod.* 2013;76(4):672–678.
23. Bottegoni G, Rocchia W, Rueda M, Abagyan R, Cavalli A. Systematic exploitation of multiple receptor conformations for virtual ligand screening. *PLoS One.* 2011;6(5):e18845.
24. Laskowski RA, Swindells MB. LigPlot+: multiple ligand-protein interaction diagrams for drug discovery. *J Chem Inf Model.* 2011;51(10): 2778–2786.
25. Salentin S, Schreiber S, Haupt VJ, Adasme MF, Schroeder M. PLIP: fully automated protein-ligand interaction profiler. *Nucleic Acids Res.* 2015;43(W1):W443–W447.
26. Wang Y, Xiao J, Suzek TO, Zhang J, Wang J, Bryant SH. PubChem: a public information system for analyzing bioactivities of small molecules. *Nucleic Acids Res.* 2009;37:W623–W633.
27. The PyMOL Molecular Graphics System, Version 1.7.4 Schrödinger, LLC [computer program]. 2015.
28. Guerois R, Nielsen JE, Serrano L. Predicting changes in the stability of proteins and protein complexes: a study of more than 1000 mutations. *J Mol Biol.* 2002;320(2):369–387.
29. Schymkowitz J, Borg J, Stricher F, Nys R, Rousseau F, Serrano L. The FoldX web server: an online force field. *Nucleic Acids Res.* 2005;33:W382–W388.
30. Trott O, Olson AJ. AutoDock Vina: improving the speed and accuracy of docking with a new scoring function, efficient optimization, and multithreading. *J Comput Chem.* 2010;31(2):455–461.
31. Seeliger D, de Groot BL. Ligand docking and binding site analysis with PyMOL and Autodock/Vina. *J Comput Aided Mol Des.* 2010; 24(5):417–422.
32. Cheng F, Li W, Zhou Y, et al. AdmetSAR: a comprehensive source and free tool for assessment of chemical ADMET properties. *J Chem Inf Model.* 2012;52(11):3099–3105.
33. Furukawa A, Arita T, Fukuzaki T, et al. Substituents at the naphthalene C3 position of (-)-cercosporamide derivatives significantly affect the maximal efficacy as PPARgamma partial agonists. *Bioorg Med Chem Lett.* 2012;22(3):1348–1351.
34. Rother K, Preissner R, Goede A, Frommel C. Inhomogeneous molecular density: reference packing densities and distribution of cavities within proteins. *Bioinformatics.* 2003;19(16):2112–2121.
35. Mirza MU, Ghori NU, Ikram N, Adil AR, Manzoor S. Pharmacoinformatics approach for investigation of alternative potential hepatitis C virus nonstructural protein 5B inhibitors. *Drug Des Devel Ther.* 2015; 9:1825–1841.
36. Borea PA, Varani K, Gessi S, Gilli P, Dalpiaz A. Receptor binding thermodynamics as a tool for linking drug efficacy and affinity. *Farmaco.* 1998;53(4):249–254.
37. Yuriev E. Challenges and advances in structure-based virtual screening. *Future Med Chem.* 2014;6(1):5–7.
38. Kitchen DB, Decornez H, Furr JR, Bajorath J. Docking and scoring in virtual screening for drug discovery: methods and applications. *Nat Rev Drug Discov.* 2004;3(11):935–949.
39. Ripphausen P, Stumpfe D, Bajorath J. Analysis of structure-based virtual screening studies and characterization of identified active compounds. *Future Med Chem.* 2012;4(5):603–613.
40. Lipinski CA. Lead- and drug-like compounds: the rule-of-five revolution. *Drug Discov Today.* 2004;1(4):337–341.
41. Danishuddin M, Khan AU. Structure based virtual screening to discover putative drug candidates: necessary considerations and successful case studies. *Methods.* 2015;71:135–145.
42. Shirai NC, Kikuchi M. Structural flexibility of intrinsically disordered proteins induces stepwise target recognition. *J Chem Phys.* 2013; 139(22):225103.
43. Shen J, Cheng F, Xu Y, Li W, Tang Y. Estimation of ADME properties with substructure pattern recognition. *J Chem Inf Model.* 2010; 50(6):1034–1041.
44. Pham-The H, González-Álvarez I, Bermejo M, et al. In silico prediction of Caco-2 Cell permeability by a classification QSAR approach. *Mol Inf.* 2011;30(4):376–385.
45. Wang Z, Chen Y, Liang H, Bender A, Glen RC, Yan A. P-glycoprotein substrate models using support vector machines based on a comprehensive data set. *J Chem Inf Model.* 2011;51(6):1447–1456.
46. Chen L, Li Y, Zhao Q, Peng H, Hou T. ADME evaluation in drug discovery. 10. Predictions of P-glycoprotein inhibitors using recursive partitioning and naive Bayesian classification techniques. *Mol Pharm.* 2011;8(3):889–900.
47. Broccatelli F, Carosati E, Neri A, et al. A novel approach for predicting P-glycoprotein (ABCB1) inhibition using molecular interaction fields. *J Med Chem.* 2011;54(6):1740–1751.
48. Kido Y, Matsson P, Giacomini KM. Profiling of a prescription drug library for potential renal drug-drug interactions mediated by the organic cation transporter 2. *J Med Chem.* 2011;54(13):4548–4558.
49. Carbon-Mangels M, Hutter MC. Selecting relevant descriptors for classification by Bayesian estimates: a comparison with decision trees and support vector machines approaches for disparate data sets. *Mol Inf.* 2011;30(10):885–895.
50. Cheng F, Yu Y, Shen J, et al. Classification of cytochrome P450 inhibitors and noninhibitors using combined classifiers. *J Chem Inf Model.* 2011;51(5):996–1011.
51. Anzenbacher P, Anzenbacherova E. Cytochromes P450 and metabolism of xenobiotics. *Cell Mol Life Sci.* 2001;58(5–6):737–747.
52. Olsen L, Oostenbrink C, Jorgensen FS. Prediction of cytochrome P450 mediated metabolism. *Adv Drug Deliv Rev.* 2015;86:61–71.
53. Lynch T, Price A. The effect of cytochrome P450 metabolism on drug response, interactions, and adverse effects. *Am Fam Physician.* 2007; 76(3):391–396.
54. OSIRIS Property Explorer. Available from: http://www.organic-chemistry.org/prog/peo/. Accessed June 29, 2015.
55. Pedretti A, Villa L, Vistoli G. VEGA: a versatile program to convert, handle and visualize molecular structure on Windows-based PCs. *J Mol Graph Model.* 2002;21(1):47–49.